Facies (2017) 63:24
DOI 10.1007/s10347-017-0505-0

ORIGINAL PAPER

Anachronistic and unusual carbonate facies in uppermost Lower Triassic rocks of the western Balkanides, Bulgaria

Athanas Chatalov[1]

Received: 3 April 2017 / Accepted: 7 July 2017 / Published online: 19 July 2017

Abstract Anachronistic and unusual carbonate facies (AUCFs) are identified in four localities with exposed Spathian strata in the western Balkanides. These include thin-bedded micritic limestone, flat-pebble breccia/conglomerate, mud-chip conglomerate, limestone-marl ribbon rock, vermicular limestone, and microbial oolite. Their depositional and/or early diagenetic origin is interpreted on the basis of petrographic characteristics, results from previous studies, and comparison with analogues from the geological record. Various controlling factors are distinguished in the context of their relative influence on global, regional, or local scale, i.e., environmental conditions (high degree of $CaCO_3$ supersaturation, fluctuations in oxygen levels and salinity), biological controls (bioturbation, microbial blooms, scarcity or abundance of metazoans), and uniformitarian sedimentary processes (wave agitation, storm action, terrigenous input, seismic shocks). Most of the AUCFs are assigned to features associated with enhanced $CaCO_3$ precipitation, while the vermicular limestones belong to fabrics that formed due to limited biologic activity. The thin-bedded micritic limestones, flat-pebble breccias/conglomerates, and limestone-marl ribbon rocks represent anachronistic facies, while the remaining AUCFs are regarded as unusual sedimentary features and fabrics. This study reports a new occurrence of diverse Spathian AUCFs formed in subtidal settings besides those described from the southwestern USA and south China. The results show that anomalous paleoceanographic conditions for carbonate sedimentation persisted locally in the shallow Western Tethys until late Early Triassic time.

Keywords Anachronistic facies · Unusual facies · Carbonate · Subtidal · Spathian · Western Tethys

Introduction

The term ‘anachronistic facies’ was introduced by Sepkoski et al. (1991) for depositional features that are abundant in Precambrian and Cambrian–Lower Ordovician rocks but become distinctly rare in younger Phanerozoic strata. Later, a great diversity of unusual sedimentary facies and fabrics was identified in Lower Triassic deposits worldwide and some of them were considered as being anachronistic in nature (Wignall and Twitchett 1999; Lehrmann et al. 2001; Pruss et al. 2005b; Baud et al. 2007; Zhao et al. 2008; Woods 2009, 2014; Li et al. 2013; Abdolmaleki and Tavakoli 2016; Deng et al. 2016). Such unusual features are known from various locations around the globe comprising a broad spectrum of lithofacies, structures, and textures: vermicular limestones, flat-pebble and mud-chip conglomerates, microbialites (including wrinkle structures in siliciclastic deposits), seafloor precipitates, giant ooids and other coated grains (see Woods 2014, and references therein), as well as ribbon rocks (Lehrmann et al. 2001), and thin-bedded and zebra limestones (Pruss et al. 2005b; Zhao et al. 2008). These sedimentary facies and fabrics are indicative of atypical paleoceanographic conditions, i.e., environmental stress and enhanced precipitation of $CaCO_3$ (Woods 2014), that were present during a long time span after the devastating end-Permian mass extinction and persisted until the early Middle Triassic in some regions (Pruss et al. 2006; Jaglarz and Uchman 2010; Luo et al. 2014).

✉ Athanas Chatalov
chatalov@gea.uni-sofia.bg

[1] Faculty of Geology and Geography, Sofia University St. Kliment Ohridski, 15 Tsar Osvoboditel Blvd, 1504 Sofia, Bulgaria

At least four episodes characterized by anomalous carbonate deposition during the Early Triassic have been distinguished, i.e., early Griesbachian, late Griesbachian–early Dienerian, Smithian and Spathian (Pruss et al. 2006; Baud et al. 2007; Mata and Bottjer 2012). Diverse Spathian anachronistic facies that formed in subtidal settings have been reported from the southwestern USA (Pruss and Bottjer 2004a, b; Pruss et al. 2004, 2005a, b; Pruss and Payne 2009; Woods 2009; Mata and Bottjer 2011) and south China (Lehrmann et al. 2001, 2012; Zhao et al. 2008, 2015; Chen et al. 2011; Ezaki et al. 2012; Luo et al. 2016). These occurrences include flat-pebble conglomerates, mud-chip facies, vermicular limestones, seafloor precipitates, various microbialites (stromatolites, thrombolites, coated grains, spheroids, wrinkle structures), giant ooids, ribbon rocks, and thin-bedded and zebra limestones.

Four 'anachronistic facies' were recently recognized in exposures of Spathian carbonate rocks from northwestern Bulgaria (Chatalov 2016). The present study documents new occurrences of the same facies and two additional types in Spathian deposits from a larger area across the western Balkanides. A detailed petrographic characterization of these unusual sedimentary features and fabrics is presented and their origin discussed. In addition, an attempt is made to distinguish between the truly anachronistic and simply unusual Lower Triassic facies.

The main purpose of this study is to report a new spectacular occurrence of diverse anachronistic and unusual carbonate facies (AUCFs) in Spathian rocks (Fig. 1). This study complements the few known examples of such facies described from Lower Triassic deposits in the Western Tethys realm, i.e., Italy, Hungary, and Turkey (Wignall and Twitchett 1999; Baud et al. 2005; Hips and Haas 2006).

Geological setting and previous work

The Balkanide facies type of the Triassic (Ganev 1974) follows the tripartite subdivision of the Triassic system in the Peri-Tethyan Germanic Basin, i.e., continental Buntsandstein, marine Muschelkalk, and continental Keuper. The entire sedimentary succession corresponds to a second-order transgressive–regressive (T–R) stratigraphic cycle controlled by a second-order eustatic cycle (Chatalov 2013). Lithostratigraphically, the Lower to Upper Triassic marine strata are referred to as the Iskar Carbonate Group, which consists of limestones, dolostones, and minor amounts of siliciclastic rocks (Tronkov 1981). According to the Alpine tectonic model for Bulgaria proposed by Ivanov (1998), this unit is exposed in the External, Intermediate and Internal Balkanides, and also occurs in the subsurface of the Moesian Platform (Fig. 2). The Iskar Carbonate Group overlies predominantly alluvial deposits of the Lower Triassic Petrohan Terrigenous Group and is covered by fluvial and playa deposits of the Upper Triassic Moesian Group. The thickness of the carbonate succession reaches up to 500 m or more in the western parts of the Balkanides. The Iskar Carbonate Group is subdivided into formal units of lower

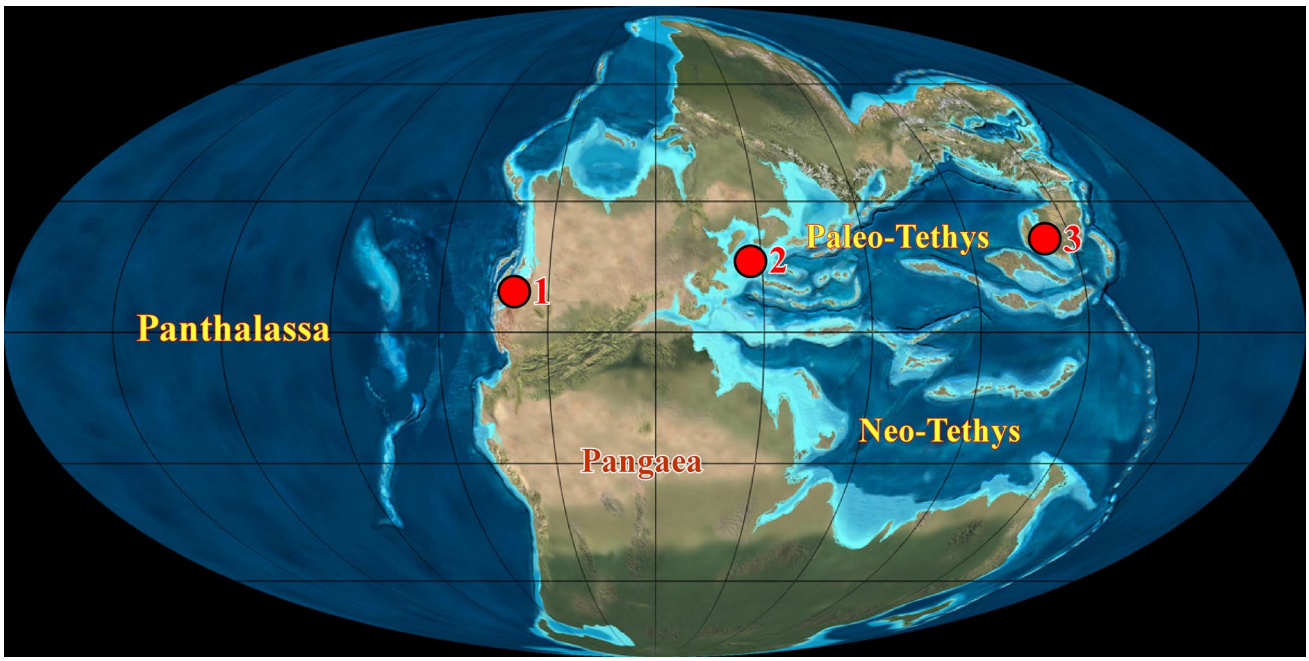

Fig. 1 Global paleogeography in the Early–Middle Triassic (from Blakey 2011) and location of the three regions with reported occurrences of diverse Spathian AUCFs. *1* southwestern USA, *2* western Bulgaria, *3* south China (see references in text)

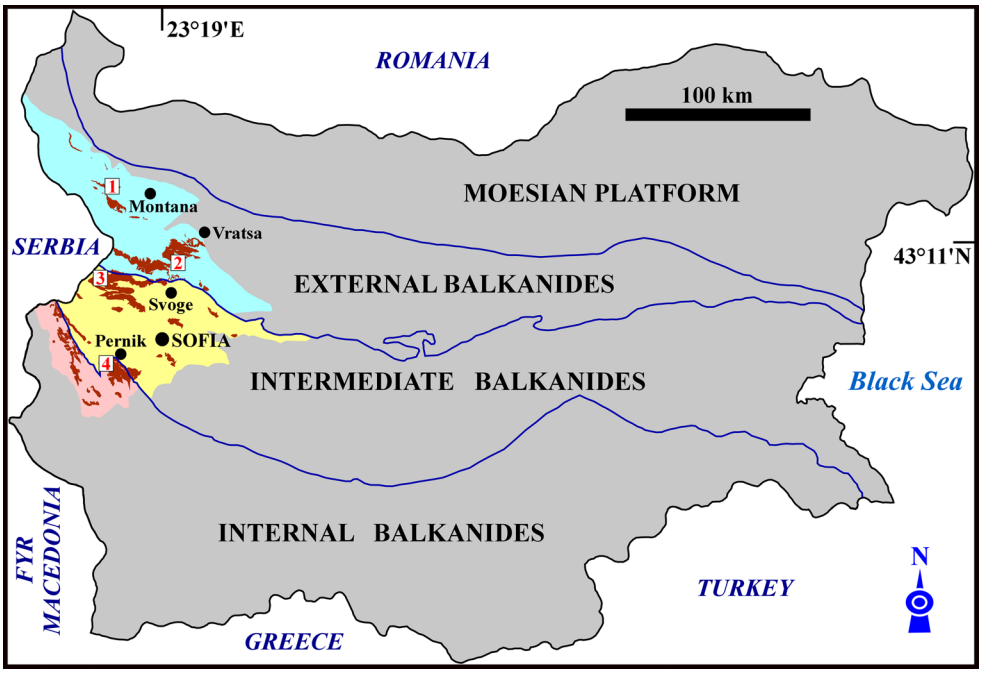

Fig. 2 Exposures of lower to upper Triassic marine sedimentary rocks, i.e., Iskar Carbonate Group (shown as *brown patches*), and the location of stratigraphic sections examined for this study with recognized Spathian AUCFs in the western Balkanides: *1* Chelyustnitsa (43°27′N, 23°0′E), *2* Iskar River gorge (43°6′N, 23°25′E), *3* Ropot–Golesh (43°2′N, 22°57′E), *4* Bela voda (42°35′N, 22°58′E), *blue*—West Balkan Zone, *yellow*—western Srednogorie Zone, *pink*—northern Kraishte Zone. The Alpine tectonic subdivision of Bulgaria is after Ivanov (1998)

rank (Formations, Members, Beds) as some of them are recognized in different tectonic zones (Fig. 3).

Biostratigraphic and sedimentological studies in the West Balkan Zone of the External Balkanides have shown that marine deposition occurred from the Spathian to the Julian (Tronkov 1968, 1973) on a homoclinal carbonate ramp, which evolved in the subtropical belt of the NW Tethys (Chatalov 2013). Diverse subtidal, intertidal and supratidal facies were formed in several depositional environments: tidal flats, inner ramp lagoons and shoals, storm-dominated and fair-weather mid-ramp areas, mid-outer ramp (slope), and storm-influenced outer ramp. Carbonate sedimentation was characterized by abundant lime mud production, intensive formation of coated grains, intraclasts and peloids,

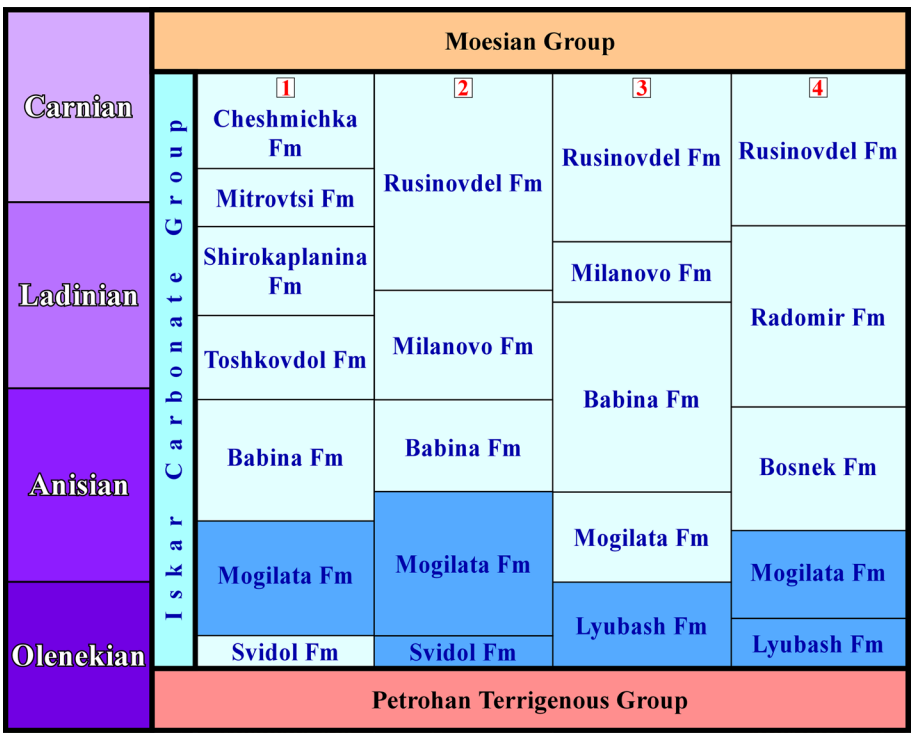

Fig. 3 Lithostratigraphic subdivision of the Iskar Carbonate Group in the four localities (based on data from Tronkov 1968, 1973, 1983; Benatov and Chatalov 2000). The formal units shown in *dark blue* contain Spathian AUCFs. Thicknesses of the lithostratigraphic units are not to scale

and precipitation of marine cements (Chatalov 2016). The development of carbonate-secreting organisms dominated by mollusks, echinoderms, brachiopods, foraminifers and cyanobacteria was not accompanied by growth of microbial build-ups or metazoan reefs. The inferred environmental constraints of the ramp depositional system include normal marine to hypersaline conditions, warm, clear water, aerobic and dysaerobic bottom conditions, a predominantly soft lime mud substrate, intensive storm activity, and periodic seismic influence (Chatalov 2013). Two main stages of ramp development (retrogradational and progradational) produced two genetic units (transgressive and regressive) separated by a maximum flooding zone (Terebratula Beds). The Triassic marine succession shows similarities to other ramp and platform carbonates deposited across the Western Tethys shelf area and in Peri-Tethys basins during the Triassic (Chatalov 2013).

Biostratigraphic data from the Iskar Carbonate Group exposed in the western sectors of the Intermediate Balkanides (western Srednogorie Zone) and Internal Balkanides (Kraishte Zone) define a chronostratigraphic range from the Spathian to the Sevatian (Tronkov 1983; Budurov et al. 1995). Sedimentological studies indicate deposition in tidal flat and shallow to deep subtidal environments, e.g., low-energy, mud-dominated lagoons and high-energy shoals (Vaptsarova 1986; Belivanova 2000; Chatalov 2002; Belivanova and Chatalov 2005). A specific feature in the evolution of the carbonate platform was the local influx of terrestrial material during the Ladinian (Čatalov 1988), between the two major deepening and shallowing stages (Belivanova 2000). The carbonate production, biota development and environmental constraints (Tronkov 1983; Vaptsarova 1986; Budurov et al. 1995; Belivanova 2000; Chatalov 2002; Belivanova and Chatalov 2005) are very similar to the Triassic marine succession in the West Balkan Zone.

Materials and methods

Twenty-six stratigraphic sections containing exposed Lower Triassic rocks were studied in the western Balkanides in order to distinguish various types of AUCFs. The rock color, stratification pattern, sedimentary structures and textures of macroscopically recognized AUCFs were described along with the distribution; size, morphology and internal fabric of carbonate clasts and trace fossils. The ichnofabric index (ii) proposed by Droser and Bottjer (1986) was used to determine levels of bioturbation in cross section and the bedding-plane bioturbation index (bpbi) of Miller and Smail (1997) was applied to record the degree of bioturbation on bedding planes. Standard thin-sections for observation with transmitted light microscopy were prepared from 43 samples of limestones, dolostones, and calcareous marls. The samples collected from oolitic carbonates allowed the identification of another type of unusual carbonate facies under the microscope. Petrographic study of depositional textures and some diagenetic alterations (allochems, matrix, siliciclastic admixtures, bioturbation, authigenic minerals) provided additional data for comprehensive interpretation of the AUCFs.

Anachronistic and unusual carbonate facies

AUCFs were identified from four localities with exposures of Lower Triassic rocks. Two of them (Chelyustnitsa, Iskar River gorge) occur in the West Balkan Zone and the other two (Ropot–Golesh, Bela voda) are located in the western Srednogorie Zone and northern Kraishte Zone, respectively (Fig. 2). These facies include thin-bedded micritic limestone, flat-pebble breccia/conglomerate, mud-chip conglomerate, limestone-marl ribbon rock, vermicular limestone, and microbial oolite. Lithostratigraphically, they belong to three formal units: the Svidol Formation, Lyubash Formation, and Mogilata Formation (Fig. 3). The vertical distribution of AUCFs in the four localities is presented in Fig. 4.

The Early Triassic age of the Svidol Fm, Lyubash Fm and intervals of various thicknesses of the Mogilata Fm is poorly constrained by biostratigraphic data; it is defined primarily on the basis of scarce Spathian macrofauna from the three units and the appearance of Anisian macrofossils, foraminifers and conodonts in the Mogilata Fm (Tronkov 1968, 1973, 1976, 1983; Budurov et al. 1995; Benatov and Chatalov 2000). The chronostratigraphic range corresponds to the Spathian substage as determined by the presence of bivalve assemblages containing *Costatoria costata* (Zenker) and the ammonoid species *Beneckeia tenui*s (Seebach). The *C. costata* Zone was proposed to denote the upper Spathian in the biostratigraphic zonation of the Western Tethyan sections based on bivalves (Broglio Loriga et al. 1990; see also Hips and Pelikán 2002). Moreover, coexistence of the two taxa was documented from Spathian strata (based on paleomagnetic data from Nawrocki and Szulc 2000) in the Polish part of the Germanic Peri-Tethys Basin (Szulc 2000).

Thin-bedded micritic limestone

Description

This widespread facies in the Lyubash Fm and Mogilata Fm is characterized by the alternation of subparallel thin beds and/or laminae consisting of dark grey and light grey micritic limestones (Figs. 5a–c, 6a). In general, the dark-colored layers appear thicker (up to 3 cm) while the light grey layers are only several millimeters thick. The former are planar to slightly undulatory, and are commonly cracked and locally disrupted. Some beds show irregularly varying thicknesses

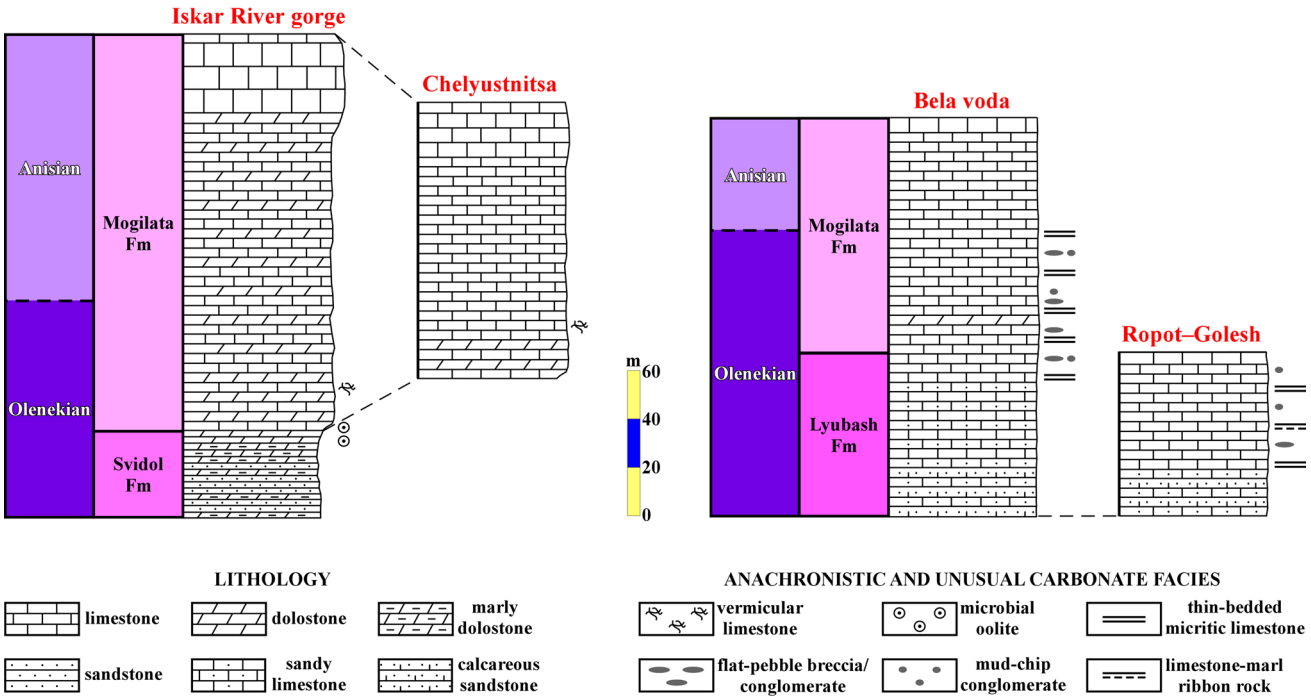

Fig. 4 Stratigraphic-lithologic logs of upper Olenekian to lower Anisian carbonate units in the four localities showing the vertical distribution of identified Spathian AUCFs

along their length without significant vertical loading into underlying beds, i.e., these beds largely resemble pinch-and-swell structure. Most limestones are completely unbioturbated (ii 1) while others exhibit high levels of bioturbation (ii 4–5); recognized trace fossils are exclusively *Planolites*. Bedding-plane bioturbation is difficult to ascertain due to the lack of discrete bedding surfaces. A distinctive feature of the thin-bedded micritic limestones is their association with flat-pebble breccias/conglomerates and mud-chip conglomerates.

A similar carbonate facies was described from the Virgin Limestone Member (Spathian) in Nevada and California (USA) under two different names, i.e., 'thin carbonate beds' (Pruss et al. 2005b) and 'thin-bedded micritic mudstones' (Mata and Bottjer 2011).

Interpretation

The abundant micrite and lack of tide-, wave-, or current-generated structures suggest deposition from suspension in a non-agitated subtidal setting (Table 1). The close association with flat-pebble breccias/conglomerates and mud-chip conglomerates indicates intermittent erosion of the seafloor (see below), which probably was in reach of major storms, i.e., near storm-wave base (see Mata and Bottjer 2011). Rapid submarine cementation and absence of deep vertical bioturbation were major prerequisites for the formation and preservation of thin micritic beds and laminae (Sepkoski et al. 1991; Wignall and Twitchett 1999; Pruss et al. 2005a, b; Woods 2009; Mata and Bottjer 2011). Such conditions at the sea floor can also explain the development of extensive, shallow-penetrating bioturbation and sediment homogenization in some deposits of this facies. The local occurrence of bed thinning and thickening, i.e., pinch-and-swell structure, is interpreted to be the result of ductile deformation, most likely triggered by earthquakes (Knaust 2002; Ettensohn et al. 2011; El Taki and Pratt 2012).

Flat-pebble breccia/conglomerate

Description

The medium-to-thick (0.7–1.2 m) limestone beds containing flat pebbles show various patterns of vertical distribution of the clasts. In the first type of flat-pebble breccia/conglomerate, dark grey pebbles are embedded in light grey micritic matrix; the top laminae of the underlying thin-bedded micritic facies are truncated (Fig. 5b). In the second variety, cm-thick lenticular layers of flat-pebble breccia/conglomerate, with uneven lower and upper boundaries, occur between vertical intervals of bioturbated (ii 3–4) thin-bedded micritic limestones (Fig. 5c). In both cases, the poorly sorted and ungraded flat pebbles are associated with variable amounts of mud chips.

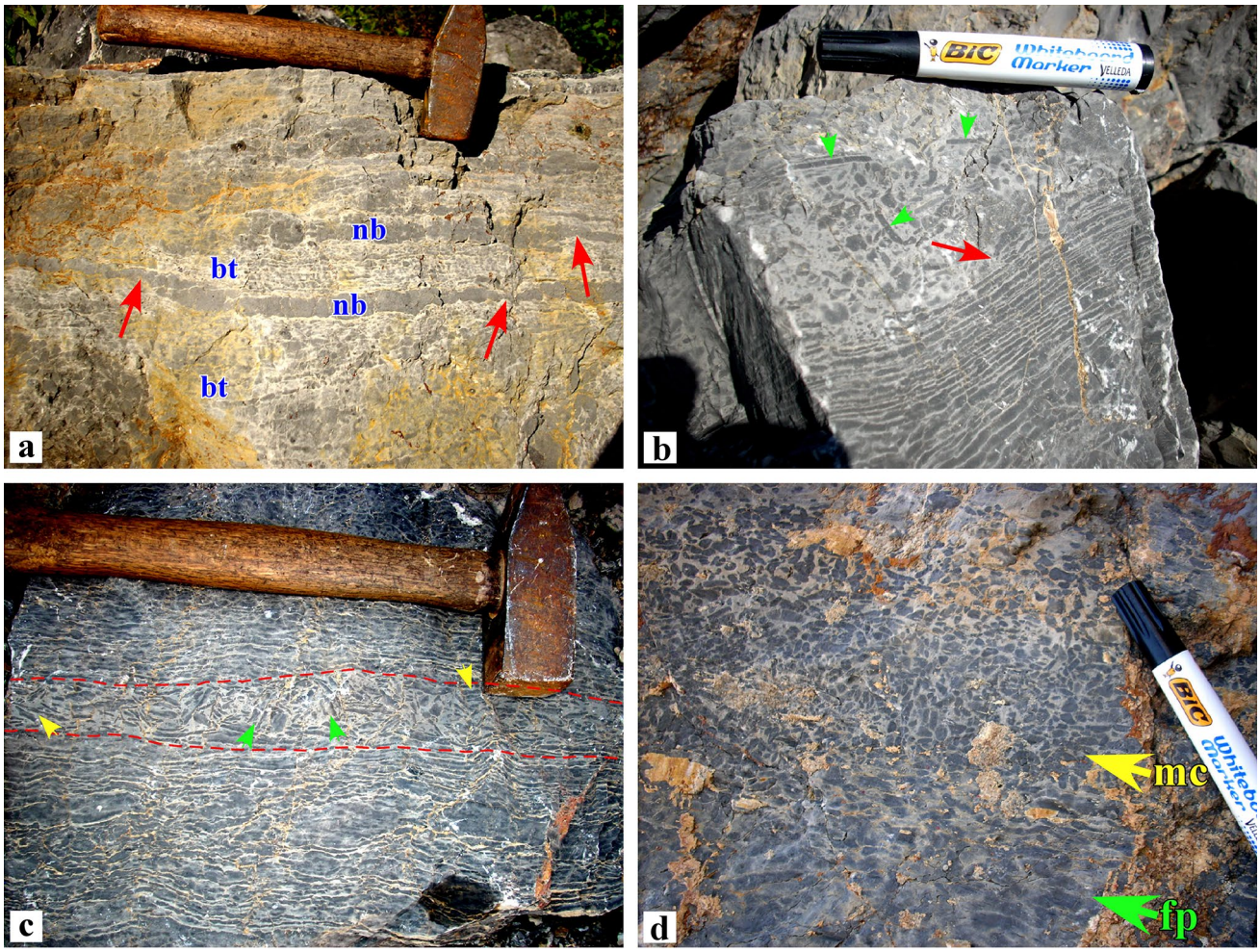

Fig. 5 AUCFs in the Mogilata Fm from the Bela voda locality. **a** Thin-bedded micritic limestone showing alternation of bioturbated (*bt*) vertical intervals (ii 3–5) and non-bioturbated (*nb*) dark grey layers (ii 1) with local development of pinch-and-swell structure (*arrows*). *Scale:* hammer is 33 cm long. **b** Same facies as a but consisting of thicker dark grey and thinner light grey beds or laminae. The upper part of the limestone bed is flat-pebble breccia/conglomerate that is clast- to matrix-supported. Note truncated lamina at the top of the thin-bedded facies (*red arrow*) and flat pebbles with high aspect ratio (*green arrows*). *Scale:* marker pen is 13.5 cm long. **c** Lenticular layer of flat-pebble breccia/conglomerate (marked by *dashed lines*) between vertical intervals of bioturbated (ii 3–4) thin-bedded micritic limestone; note the predominantly random clast orientation with local occurrences of imbricated (*yellow arrows*) and edgewise (*green arrows*) fabrics. **d** Flat-pebble breccia/conglomerate (*fp*) grading upwards into mud-chip conglomerate (*mc*); the clasts show diminishing size, lower aspect ratio, higher degree of roundness, better sorting, and sharp outlines against the matrix as they pass upwards from the flat-pebble breccia/conglomerate to the mud chip facies

Elsewhere, flat-pebble breccia/conglomerate grades upwards into mud-chip conglomerate as the clasts show diminishing size, lower aspect ratio, higher degree of roundness, better sorting, and sharp outlines against the matrix (Fig. 5d). The length of the flat pebbles ranges from several mm (a few clasts are granule size) to about 4 cm; their width reflects the thickness of the dark grey layers in the thin-bedded micritic limestones. The clast morphology is dominantly tabular, and is characterized by angular or rounded edges (larger clasts are more angular). The texture of the flat-pebble breccia/conglomerate varies from clast-supported to matrix-supported and a transition between the two may be observed vertically or laterally within a single bed. The clast orientation is mostly random, with local occurrences of imbricated and/or edgewise fabrics. Under the microscope, the flat pebbles display very similar texture and only a slight color difference relative to the surrounding micritic matrix, seemingly due to lesser amounts of clay admixtures. The rocks contain rare skeletal remains (ostracods, foraminifers, bivalves) and silt- to fine sand-sized detrital grains (predominantly quartz).

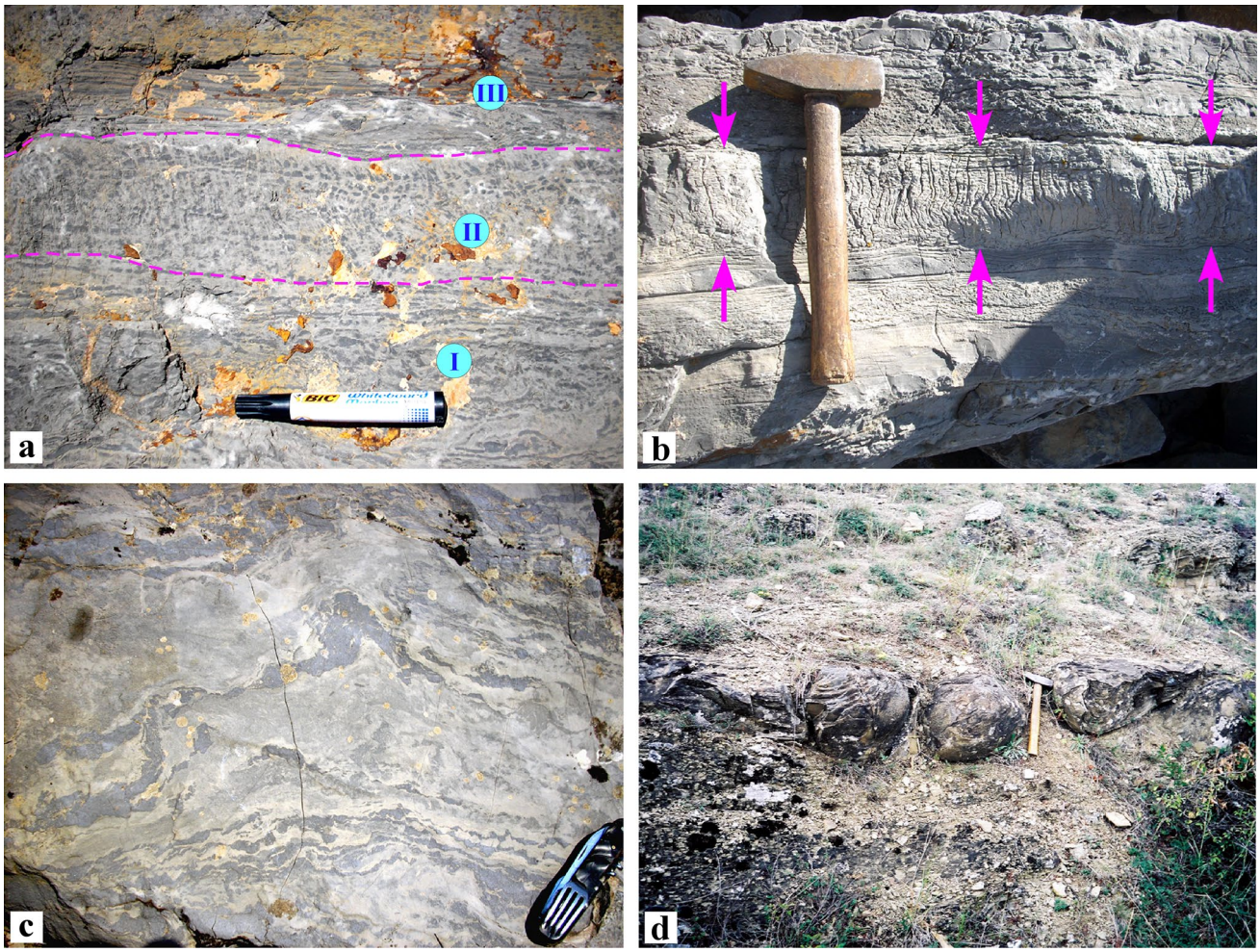

Fig. 6 Deformation structures interpreted as seismites in the Mogilata Fm from the Bela voda locality (**a**–**c**) and the Lyubash Fm from an exposure near the Ropot–Golesh locality (**d**). **a** Bioturbated layer with poorly preserved sigmoidal shear surfaces (*dashed lines*, interval *II*) between the overlying and underlying layers (intervals *I* and *III*) showing variable disruption by bioturbation (ii 1–4) in the thin-bedded micritic limestones. **b** Bed of micritic limestone (marked by *arrows*) having distinct sigmoidal shear surfaces. **c** Various folds with local appearance of pinch-and-swell structure in micritic limestone. *Scale:* pocket knife is 8.5 cm long. **d** Ball-and-pillow structure developed in calcareous sandstone bed overlying calcareous marls

Similar examples of flat-pebble breccias/conglomerates were reported in studies of Lower Triassic carbonate deposits from the USA, Italy, Turkey, Iran, and China (Wignall and Twitchett 1999; Pruss et al. 2005b, 2006; Zhao et al. 2008; Woods 2009; Abdolmaleki and Tavakoli 2016).

Interpretation

Carbonate flat-pebble breccias/conglomerates are intraformational rudstones or floatstones that can be formed in shallow to deep subtidal (Wignall and Twitchett 1999) and intertidal to supratidal settings (Demicco and Hardie 1994). Subtidal flat pebbles are commonly produced as the result of rapid lithification of the seafloor and subsequent rip-up and reworking by storm events (Sepkoski et al. 1991; Chatalov and Vangelov 2001; Myrow et al. 2004; Pruss et al. 2005b; Mata and Bottjer 2011; among others). Other mechanisms proposed in the literature include seismically induced mass movements (Kullberg et al. 2001), early diagenetic deformation and subsequent mobilization triggered by external forces (Chen et al. 2009), tsunami waves (Łuczyński et al. 2014), and internal waves (Abdi et al. 2014).

In this case, the lack of desiccation cracks, tepees, fenestrae and spar-filled nodules is inconsistent with an intertidal/supratidal origin of the breccias/conglomerates. Gravity-driven mass movements can be ruled out as a formation mechanism by the absence of associated deformation structures and lithofacies indicating a slope environment (e.g., slumps, slides, sediment-gravity-flow deposits). Early diagenetic deformation with subsequent mobilization is also unlikely because of the lack of interbedded lithologies such as marlstone or shale, layers with contrasting texture such as

Table 1 Interpretation of the Spathian anachronistic and unusual carbonate facies (AUCFs)

AUCF	Mechanism of formation	Depositional environment	Major controls
Thin-bedded micritic limestone	Suspension settling of lime mud	Low-energy, shallow subtidal, below FWWB above SWB	Rapid seafloor cementation, absence of deep vertical bioturbation
Flat-pebble breccia/conglomerate	Erosion and reworking by storm-induced currents and/or waves	Shallow subtidal, below FWWB above SWB	Storm activity, rapid seafloor cementation, absence of deep vertical bioturbation, early deformation by seismic shocks
Mud-chip conglomerate	Erosion and prolonged reworking by storm-induced currents and/or waves	Shallow subtidal, below FWWB above SWB, locally elevated salinity	Storm activity, rapid seafloor cementation, absence of deep vertical bioturbation
Limestone-marl ribbon rock	Suspension settling of lime mud and siliciclastic mud	Low-energy, shallow subtida below FWWB above SWB	Rapid seafloor cementation, absence of deep vertical bioturbation, terrigenous input, differential consolidation
Vermicular limestone	Moderate to intense burrowing activity of shallow infaunal organisms	Low-energy, shallow subtidal below FWWB above SWB	Bioturbation, rapid seafloor cementation, shifting environmental conditions (oxygen levels and/or salinity)
Microbial oolite	Microbially mediated precipitation of micrite	High-energy, very shallow subtidal, above FWWB	Enhanced precipitation of $CaCO_3$, microbial bloom, wave agitation

grainstone, and gradual transition from undisturbed rock to clast-bearing intervals (see Chen et al. 2009). Although simple criteria for identification of tsunamites do not exist (Goff et al. 2012), the lack of evidence for a catastrophic high-energy event with onshore transport of redeposited material and the limited area of occurrence of the flat-pebble breccias/conglomerates precludes a tsunami origin. Lastly, no diagnostic criteria for internal-wave deposits can be recognized such as a distinguishing lateral configuration, vertical architectural elements and sedimentary structures (Bádenas et al. 2012; Abdi et al. 2014).

The most plausible interpretation is erosion and reworking by storm-induced currents and/or waves in a subtidal environment below fair-weather wave base. This conclusion is corroborated by the truncation of underlying thin-bedded micritic facies and the presence of lenticular interlayers with erosive bases suggesting short-lived, high-energy events. Another evidence in support of a storm-related origin is the random clast orientation with the local occurrence of imbricated and/or edgewise fabrics (Mount and Kidder 1993). The close association with thin-bedded micritic limestones indicates the influence of powerful storms that scoured incipient lithified beds/laminae of the overlying unlithified lime mud. The common angular morphology and absence of deformation of the tabular clasts also attests to rapid cementation of the subsequently eroded thin-bedded micritic sediments. Enhanced cementation of the seafloor was coupled with reduced levels of vertical bioturbation that likewise favored the formation of flat-pebble breccias/conglomerates (Sepkoski et al. 1991; Wignall and Twitchett 1999; Myrow et al. 2004; Pruss et al. 2005b, 2006; Wright and Cherns 2016). The poor sorting and diverse morphology of the clasts reflect various degrees of pre-storm lithification and/or the initial size of the flat pebbles, but may also have resulted from multiple storm events that reworked clasts that had been ripped up earlier. The current interpretation is consistent with the pronounced influence of storms during the Anisian as evidenced from studies of mid-ramp to outer ramp facies in the West Balkan Zone (Chatalov and Vangelov 2001; Chatalov 2013, 2016).

The common cracking and local disruption of dark grey layers without traces of bioturbation suggests that differential consolidation and early deformation of the dark- and light-colored beds/laminae occurred, facilitating the formation of flat pebbles during subsequent storm events. Several endogenic and exogenic mechanisms may have caused soft-sediment and/or brittle deformation of the carbonate layers. Storm-wave loading or seismic shock are the most likely triggers in the present case because there is no evidence for high sedimentation rate, tide-influenced deposition, tsunami waves, or rapid sea-level changes. Early deformation due to paleoseismic activity is implied by the occurrence of pinch-and-swell structures, sigmoidal shear surfaces and

convolute folds in the thin-bedded micritic facies (Fig. 6a) and other limestone beds (Fig. 6b, c). Sigmoidal shear surfaces are common in Lower to Middle Triassic carbonate deposits of the NW Tethys and Peri-Tethyan basins, and are usually interpreted to be the result of earthquakes (e.g., Knaust 2000; Rychliński and Jaglarz 2016). Simple folds and convolute lamination in carbonate rocks have been defined as products of hydroplastic deformation triggered by seismic activity (Knaust 2000; Ettensohn et al. 2011) if other mechanisms (sediment loading, slumping, shearing by currents) can be excluded, such as in this case. Additional evidence comes from the West Balkan Zone and the western Srednogorie Zone, where various types of seismites were reported from the Svidol Fm, Lyubash Fm and the Spathian part of the Mogilata Fm (Chatalov 2000, 2013; Chatalov et al. 2015).

Mud-chip conglomerate

Description

The mud chips and flat pebbles in the Mogilata Fm have an identical color and texture, but the former show irregular, oval or subspherical shapes, a smaller mean size (up to 1.8 cm), subrounded to well-rounded morphology, moderate sorting, and sharp outlines against the light grey micritic matrix. Mud chips are a locally dominant clast type forming thin interlayers and/or isolated occurrences within the thin-bedded micritic limestones (Fig. 7a). The mud-chip conglomerate grades upwards from underlying flat-pebble breccia/conglomerate, and exhibits an upwards transition from a clast-supported to mud-supported texture, normal grading, and a tendency to shift to a more isometric clast shape (Fig. 7b). In the Lyubash Fm, the same facies is likewise associated with thin-bedded limestones and flat-pebble breccias/conglomerates, but more commonly forms discrete thin to medium (10–40 cm) beds with a clast-supported texture (Fig. 7c). A specific feature of these beds is lack of vertical changes in the chip abundance, size and shape. Elsewhere, a mud-supported texture with moderately sorted clasts is observed on the bedding planes (Fig. 7d). In thin-sections, the mud chips display distinct boundaries and have the same internal texture as the flat pebbles. While the rocks from both units are almost devoid of bioclasts and siliciclastic grains, some mud-chip conglomerates of the Lyubash Fm contain scarce calcite pseudomorphs after gypsum/anhydrite (Fig. 7f, g).

A very close analogue of the mud-chip conglomerate in the Mogilata Fm was described from the Virgin Limestone Mb in Nevada and California (Pruss et al. 2005b; Woods 2009).

Interpretation

The intimate association of mud chips and flat pebbles in the Mogilata Fm clearly indicates that both clast types shared the same autochthonous source, i.e., the chips originated from semi-consolidated lime mud layers of the thin-bedded micritic facies that were ripped up by storms. The diverse, rounded shapes and smaller dimensions compared to the flat pebbles suggest different initial sizes and morphologies of the mud-chip intraclasts, which may have been eroded from less lithified (Pruss et al. 2005b) and/or bioturbated lime mud layers, but also from carbonate layers affected more intensely by soft-sediment to brittle deformation. Alternatively, the mud chips may have been produced through additional reworking of flat pebbles (Pruss et al. 2005b), for example, as the result of multiple storms. The last explanation is particularly applicable for the mud-chip conglomerate that grades from underlying flat-pebble breccia/conglomerate in the Mogilata Fm, or forms discrete beds in the Lyubash Fm. In this case, the diminished size, more isometric shape, better sorting and higher degree of roundness relative to the flat pebbles imply prolonged reworking of the intraclasts on the seafloor probably by storm waves. The upwards transition from clast-supported to mud-supported texture with normal grading in mud-chip conglomerates of the Mogilata Fm specifically reflects waning storm conditions. The rare calcite pseudomorphs after sulfate mineral in some rocks of the Lyubash Fm indicate a locally restricted environment with elevated salinity.

Limestone-marl ribbon rock

Description

This rare facies in the Lyubash Fm occurs as a 60-cm-thick bedset of alternating grey micritic limestones and ochre-colored calcareous marls (Fig. 7e). The planar limestone beds have a maximum thickness of 1.7 cm and a massive structure. The beds are cracked to various degrees and some are disrupted, discontinuous, or pinch out. The marl beds are consistently thicker (2–8 cm) and may contain clasts that appear identical to the limestone layers in terms of color and texture. These poorly sorted clasts are pebble-sized (0.4–1.3 cm), have diverse shapes (irregular, oval, tabular, subspherical), subangular to rounded morphology, and a random orientation. Their abundance conspicuously increases in those marl intervals that are adjacent to discontinuous, pinching-out and/or disrupted limestone beds. Under the microscope, the limestones display a mudstone texture composed of microspar and/or micrite (Fig. 7h). The calcareous

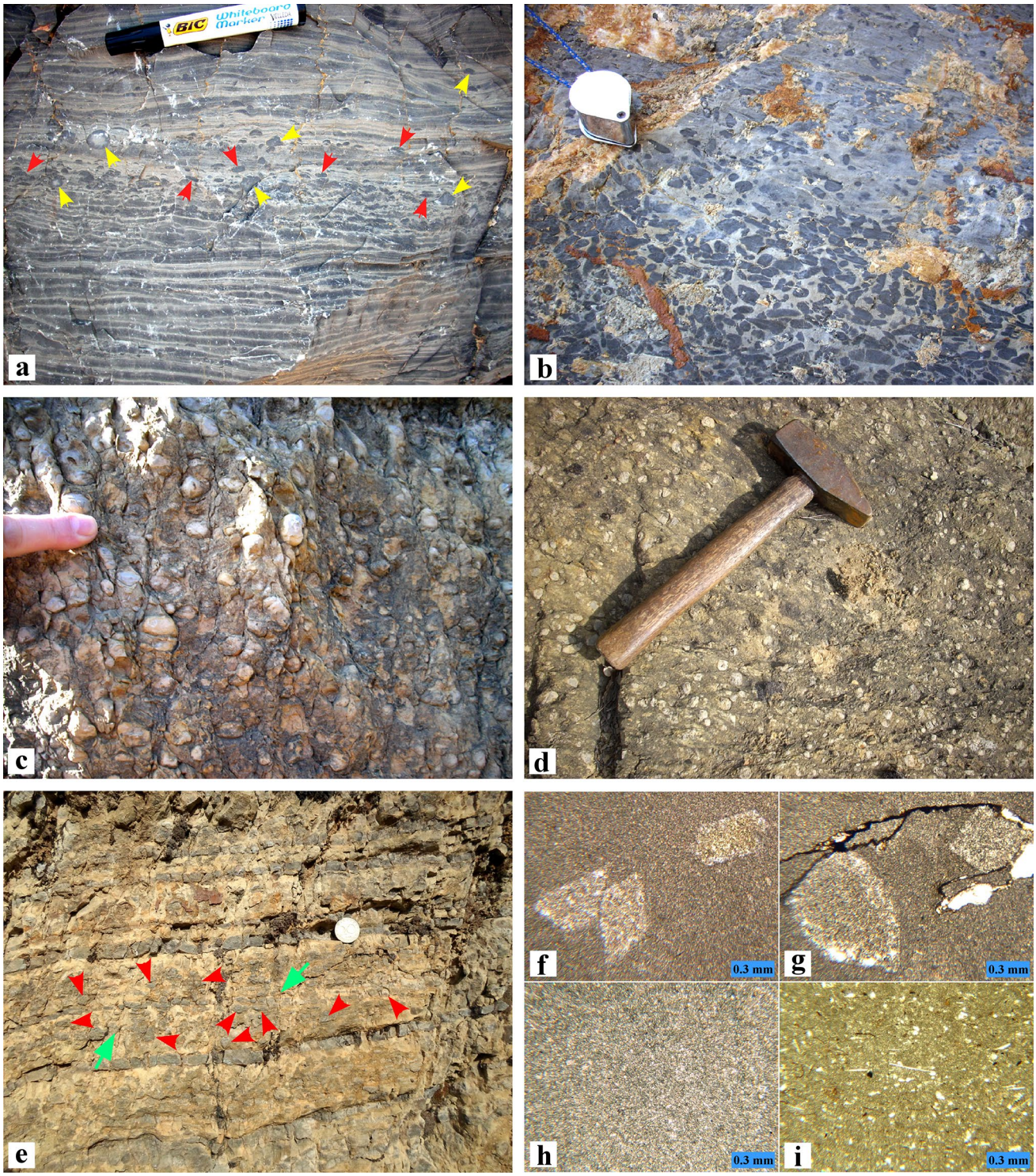

marls consist of a mixture of micrite, clay minerals, and silt- to fine sand-sized detrital grains dominated by quartz and muscovite (Fig. 7i).

The limestone-marl facies largely resembles some ribbon rocks (i.e., thinly bedded alternations of carbonate and argillaceous deposits) documented from Cambrian strata in east and north China (Chen et al. 2009, 2010; Myrow et al. 2015), northern Iran (Bayet-Goll et al. 2015), and the Argentine Precordilera (Gomez and Astini 2015).

Interpretation

Limestone-marl alternations (also named calcareous rhythmites) have been recorded in rocks of different ages in a

◂**Fig. 7** AUCFs in the Mogilata Fm from the Bela voda locality (**a**, **b**) and the Lyubash Fm from the Ropot–Golesh locality (**c**–**i**). **a** Dominant mud chips (*yellow arrows*) and subordinate flat pebbles (*red arrows*) forming a thin layer as well as isolated occurrences in thin-bedded micritic limestone; note the identical color and texture but different size and morphology of the clasts. **b** Mud-chip conglomerate showing upwards transition from clast- to mud-supported texture, normal grading, and some tendency to a more isometric clast shape. *Scale:* hand lens is 4.5 cm long. **c** Cross section of a discrete bed of mud-chip conglomerate with clast-supported texture; note the lack of vertical changes in the amount, size and shape of the clasts. **d** Bedding plane of the same facies showing matrix-supported texture with moderately sorted mud chips. **e** Limestone-marl ribbon rock composed of alternating grey micritic limestones and ochre-colored calcareous marls. The limestone layers are commonly cracked and locally disrupted. The marl beds contain poorly sorted limestone clasts (*red arrows*) whose amount increases close to discontinuous and/or pinching-out limestone beds (*green arrows*). *Scale:* coin diameter is 20.5 mm. **f, g** Photomicrographs of calcite pseudomorphs after gypsum/anhydrite that exhibit lenticular, lozenge and axehead forms in mud-chip conglomerate. **h** Photomicrograph of limestone from the ribbon rock facies that displays mudstone texture. **i** Photomicrograph of calcareous marl from the same facies that consists of a mixture of micrite, clay minerals, and silt- to fine sand-sized detrital grains. All photomicrographs are in plane-polarized light

wide spectrum of depositional environments (e.g., Einsele and Ricken 1991; Colombié et al. 2012; Gomez and Astini 2015). Their origin remains controversial especially regarding the problem of primary deposition versus secondary modification (i.e., by differential diagenesis), and resolving this requires detailed studies (Westphal et al. 2010). Primary deposition is controlled by environmental changes due to various extrinsic and/or intrinsic factors (see Einsele and Ricken 1991; Westphal et al. 2010). In particular, limestone-marl ribbon rocks are usually interpreted as low-energy, subtidal sediments deposited below fair-weather wave base by suspension settling of lime and siliciclastic mud in varying proportions (Chen et al. 2010; Bayet-Goll et al. 2015; Gomez and Astini 2015; Myrow et al. 2015). In the present case, the lack of depositional structures indicating high-energy conditions and the matrix-dominated rock textures are consistent with such an interpretation. The thicker marl beds suggest periodic changes in the supply of terrigenous material, probably reflecting climate fluctuations. Rapid cementation of the seafloor and absence of bioturbation most likely favored preservation of the limestone layers. The common development of cracks with local disruption of these beds indicates differential consolidation and ductile to brittle deformation. Such early deformation is typical for indurated beds (e.g., early lithified carbonates), alternating with liquefied thixotropic layers (e.g., marls or shales), and may produce so called autoclastic breccias as a result of earthquake shocks (Montenat et al. 2007). The discontinuous and pinching-out limestone beds associated with concentrations of limestone clasts in the adjacent marl beds suggest local in situ fragmentation of early lithified lime mud layers and further re-orientation and rounding of the generated clasts. These successive stages were collectively named autoconglomeration by Chough et al. (2001) and interpreted as resulting from compaction, fluidization, and expulsion of pore water. Chen et al. (2009, 2010) claimed that initial deformation is caused by an external triggering force (e.g., seismic shock or storm-wave loading); subsequent mobilization of the clasts occurs under the influence of compaction and/or an external triggering force; and, the ultimate formation of limestone 'pseudoconglomerates' takes place under conditions of progressive burial and cementation. The clasts become rounded after fragmentation due to abrasion by other mobile clasts, attrition of fluidized flow, and/or surface tension of carbonate mud (Chough et al. 2001; Chen et al. 2009). The influence of earthquakes as a triggering force in the early deformation of the Spathain limestone-marl ribbon rocks is implied by the presence of load structures, i.e., pseudonodules, load casts and ball-and-pillow structure (Fig. 6d), in both siliciclastic and carbonate strata of the Lyubash Fm from the Ropot–Golesh locality and nearby exposures (see Chatalov 2000).

Vermicular limestone

Description

The rocks of this facies represent medium- to thick-bedded (0.4–0.7 m), dark grey mudstones showing moderate to intense bioturbation. Vermicular limestones alternate with non-bioturbated mudstones and bioclastic wackestones having massive or laminated structures. The vermicular appearance is characterized by darker, predominantly worm-like trace fossils with positive and negative reliefs on weathered rock surfaces (Fig. 8a). The densely packed and commonly intersecting vermiform bodies are concentrated on upper bedding planes and are surrounded by light-colored micritic or marly matrix (Fig. 8b). Lateral transitions to regions with a lower degree of bioturbation can be seen in some beds where the trace fossils occur as isolated vermiform bodies and irregular mottles (Fig. 8c). Surface coverage by the trace fossils varies from approximately 40 to >90%, thus corresponding to a bpbi of 4 (40–60% disruption) to 5 (60–100% disruption). Morphologically, the burrows are mostly straight, slightly curved and tongue-like but also J-shaped, U-shaped, and Y-shaped. They are horizontal to oblique to bedding planes, circular to elliptical in cross section, unlined or rarely lined, and smooth to irregularly walled. The discrete trace fossils have various lengths (up to 6.5 cm) and widths (up to 1.9 cm), and the measured maximum diameter is 1.4 cm. These macroscopic characteristics allow recognition of three ichnotaxa, i.e., *Planolites*

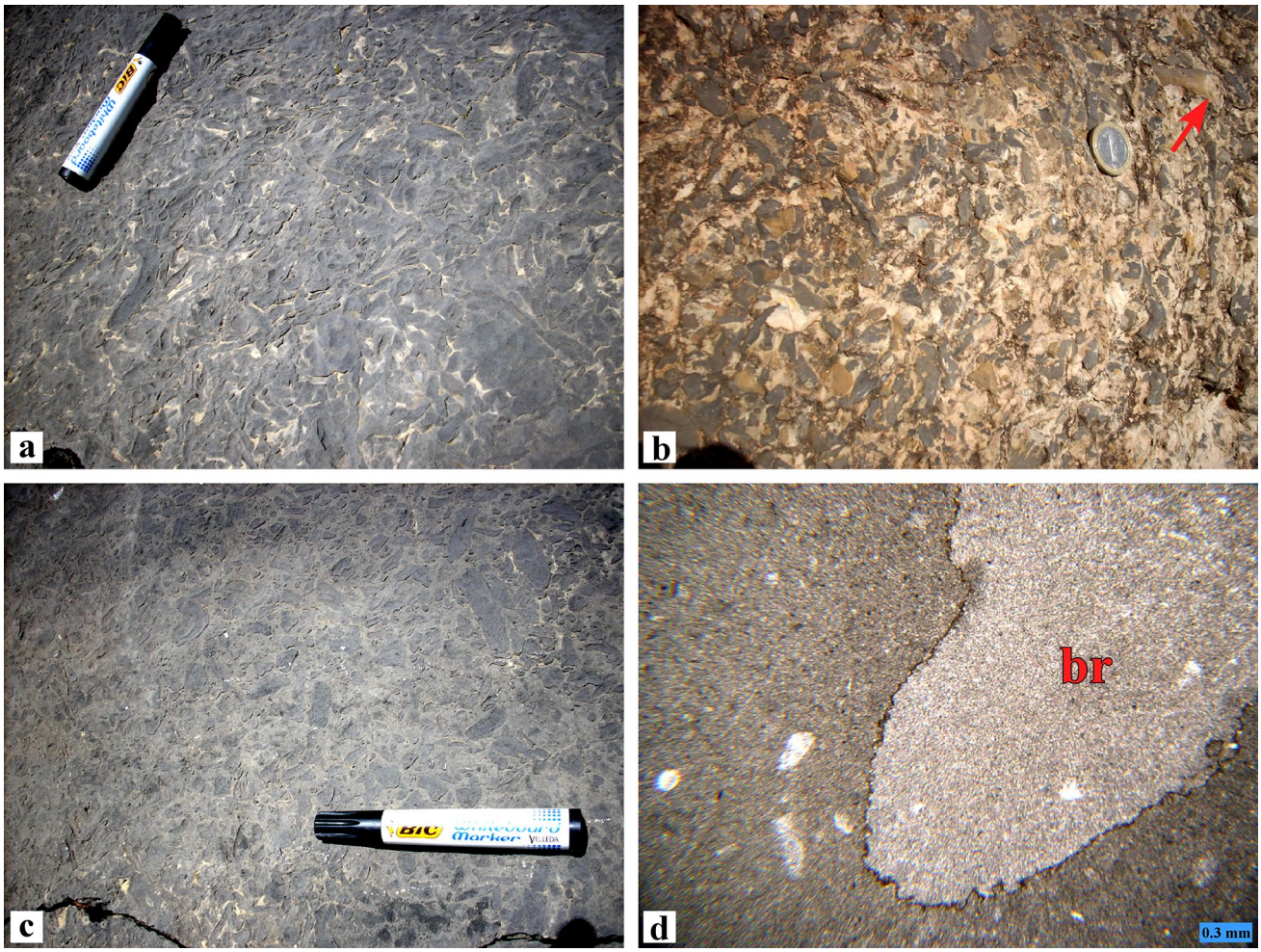

Fig. 8 Vermicular limestones in the Mogilata Fm from the Chelyustnitsa locality (**a**, **c**, **d**) and the Iskar River gorge locality (**b**). **a** High surface coverage by trace fossils (bpbi 5) that display a *dark color*, various sizes and shapes, a horizontal orientation to the bedding plane, and mostly negative relief. **b** Densely packed trace fossils (bpbi 5) showing positive relief within light-colored marly matrix. *Arrow* indicates burrow with a circular cross section. *Scale:* coin diameter is 24.5 mm. **c** Medium surface coverage by trace fossils (bpbi 4), which occur as isolated vermiform bodies and irregular mottles. **d** Photomicrograph showing burrow (*br*) with structureless micritic infill surrounded by more clayey micritic matrix. Plane-polarized light

(dominant), *Thalassinoides* and *Rhizocorallium*. In thin-sections, most vermicular micritic bodies appear structureless (Fig. 8d) while others locally display a peloidal texture. The surrounding micritic matrix is more clayey and may form a dark halo. Small amounts of silt-sized detrital grains in the matrix are dominated by quartz, and skeletal fauna are represented by very scarce ostracod shells. Isolated calcite pseudomorphs, such as those described in the mud-chip conglomerates, occur in some samples.

Vermicular limestones with similar characteristics were reported from Lower Triassic (Pruss and Bottjer 2004a; Pruss et al. 2005b; Zhao et al. 2008, 2015; Chen et al. 2011; Abbassi et al. 2015; Deng et al. 2016) and Middle Triassic strata worldwide (Jaglarz and Uchman 2010).

Interpretation

Different mechanisms of formation have been proposed to explain the origin of vermicular limestones (Zhao et al. 2008; Woods 2014; Deng et al. 2016, and references therein). In the present case, the vermicular appearance is clearly related to the burrowing activity of shallow infaunal organisms. The recognized trace fossil assemblage (*Planolites*, *Thalassinoides*, *Rhizocorallium*) can be ascribed to the *Cruziana* ichnofacies, which is characteristic of muddy subtidal substrates (softgrounds) in shallow-marine settings between fair-weather wave-base and storm wave-base, commonly in a moderate to low-energy system (MacEachern et al. 2007). The burrows represent dwelling and feeding traces (active,

structureless fill) of deposit- and suspension-feeding mobile benthos. An important control on the formation and preservation of the vermicular limestones was enhanced lithification of the seafloor, which allowed horizontal burrowing but prevented vertical bioturbation (i.e., Zhao et al. 2008; Woods 2009). The association of vermicular rocks with non-bioturbated mudstones, the common lateral transitions to less bioturbated deposits and the simple ichnofossil assemblage with subhorizontal, small-sized burrows, may indicate shifting environmental conditions, such as fluctuations in oxygen levels that limited the intensity of bioturbation (Pruss et al. 2005b). Deposition under dysoxic conditions in a restricted, low-energy setting is inferred from some facies characteristics in the lower part of the Mogilata Fm, e.g., dark rock colors, well-preserved laminations, and mudstone textures. Environmental stress may have also been due to elevated salinity (see Jaglarz and Uchman 2010), which is implied by the impoverished ichnoassemblage, presence of calcite pseudomorphs after sulfate minerals, scarcity of low-diversity benthic fauna in the vermicular limestones and adjacent carbonate beds, and the presence of peritidal dolomites indicative of a warm and dry climate (Chatalov 2016).

Microbial oolite

Description

A thick dolostone bed in the upper part of the Svidol Fm and a thick limestone bed at the base of the Mogilata Fm are oolitic grainstones or packstones with a cross-bedded structure. Mimetic dolomitization of the cortical fabric characterizes coated grains in the lower oolite bed. The ooids from both units range from subspherical to ellipsoidal in shape and are typically 0.35–0.80 mm in diameter. The ooid cortices are composed of fine-grained carbonate showing internal fabric that varies from distinctly concentric (Fig. 9a) to homogeneous and cloudy, and are commonly dark-colored with local concentrations of authigenic pyrite (Fig. 9b). Micrite and microspar laminae alternate within the concentric ooids, having equal or near equal thicknesses (from several μm to 20 μm). In some allochems, laminae become less evident in certain parts of the cortex, or disappear laterally (Fig. 9c). The ooid cortices have a diffuse or sharp contact with the nuclei, which may include peloids, micritic intraclasts, small bioclasts, or blocky calcite crystals. Asymmetric (Fig. 9d) and deformed ooids (Fig. 9e) are very common, and two or more ooids are locally cemented together to form aggregate grains with the binding material a homogeneous micrite (Fig. 9f). A specific component of the oolites are mudstone intraclasts with envelopes (Fig. 9g) that consist of dense and cloudy to finely laminated micrite. These allochems are defined as cortoids that have constructive envelopes, which is based on the following evidence (see also Woods 2013): (1) the envelopes build out from the grain surface; (2) the contact between the coating and the intraclast is smooth; (3) the envelopes show uneven thickness, being thicker on one side of the substrate grain; and, (4) the micrite in the envelopes is very similar to the micrite forming the ooid cortices. These characteristics rule out the alternative explanation for the micrite envelopes as products of destructive micritization by microborers.

The described ooids are similar to the normal-sized (≤2 mm) micritic ooids reported from Lower Triassic strata in the USA, Hungary, Turkey and China (Haas et al. 2004; Baud et al. 2005; Li et al. 2013; Woods 2013; Fang et al. 2017). The allochems with constructive envelopes greatly resemble some cortoids documented from the Virgin Limestone Mb (Woods 2013).

Interpretation

Recently, there has been growing evidence for significant microbial controls on ooid formation based on experimental work and actualistic studies (see Li et al. 2017, and references therein). Microbially mediated precipitation of $CaCO_3$ and/or constructive roles played by microbes have been assumed to be essential for the formation of some Lower Triassic micritic ooids (Woods 2013; Fang et al. 2017; Li et al. 2017). The described Spathian ooids were formed in a very shallow subtidal setting under high-energy conditions, which is inferred from the cross-bedded structure, good sorting of the ooids, abundance of intraclasts, and the winnowed texture of the oolites. Microbially mediated precipitation of micrite in the ooid cortices is supported by several lines of evidence (see also Woods 2013): cloudy, dense micrite forms the cortices of homogeneous ooids; laminae become less distinct or disappear laterally in some ooid cortices; asymmetric ooids and aggregate grains bound by micrite are locally abundant; and, the ooids are associated with cortoids that have constructive envelopes. Furthermore, the dark-colored laminae and fine-grained pyrite may indicate incorporation of organic matter into the ooid cortices, while the high amount of deformed ooids implies the presence of soft and/or semi-lithified, organic-rich nuclei. No evidence is found to support other possible origins of the ooids such as complete destructive micritization, alteration of aragonite ooids via transformation to calcite micrite, random accretion of micrite crystals in environments with low sedimentation rates, or in situ growth within microbial mats (see Flügel 2004). Some variations in the micritic ooids (concentric vs. homogeneous cortex, subspherical vs. asymmetric shape) and associated allochems (relative amount of cortoids and aggregate grains) are presumably related to differing hydrodynamic conditions, variable supply of nuclei and ooid growth rate,

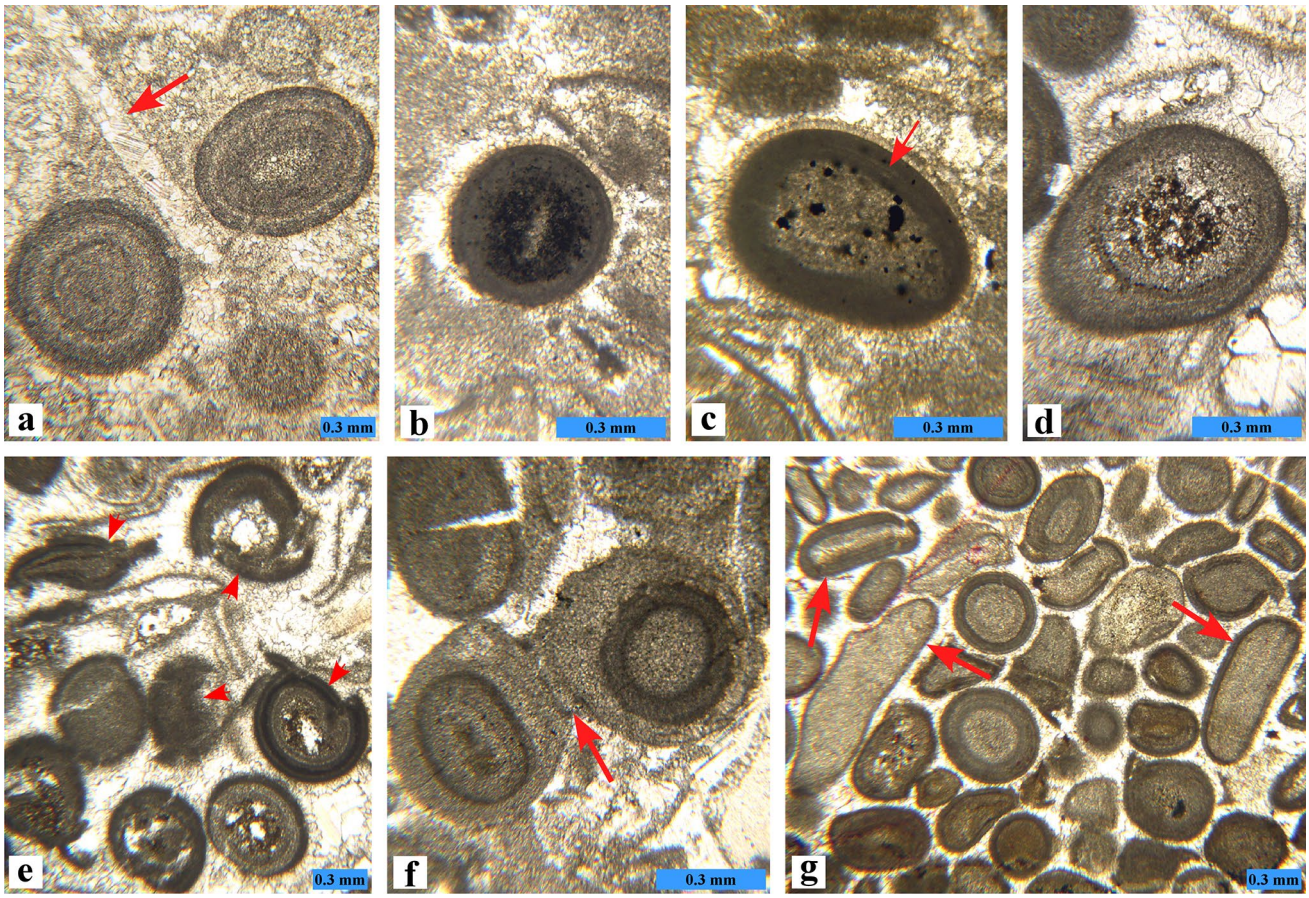

Fig. 9 Microbial ooids and cortoids from the Svidol Fm (**b**, **c**, **e**–**g**) and the Mogilata Fm (**a**, **d**), Iskar River gorge locality. Allochems in the Svidol Fm are mimetically dolomitized. **a** Subspherical and ellipsoidal ooids with distinctly concentric cortices with alternating individual micrite and microspar laminae of nearly equal thicknesses; note the lack of micritic rim around the bivalve shell (*arrow*) precluding destructive micritization of the ooid cortices. **b** Ooid with homogeneous, dark-colored cortex composed of dense, cloudy micrite; black material consists of fine pyrite crystals. **c** Ooid having the same type of cortex as b; note that some laminae are evident only in certain areas of the cortex (*arrow*), which has diffuse contact with the nucleus. **d** Asymmetric ooid; note that the additional micrite that was added to the cortex is homogenous and dense. **e** Micritic ooids showing deformed cortices (*arrows*). **f** Two asymmetric ooids bound together by homogeneous micrite (*arrow*) to form aggregate grain. **g** Mudstone intraclasts having uneven coatings of dense, cloudy to finely laminated micrite (*arrows*). These allochems are defined as cortoids with constructive microbial envelopes (for explanation see text). All photomicrographs are in plane-polarized light

and/or differences in the nature of microbial communities that caused micrite precipitation (Woods 2013). The constructive envelopes around intraclasts originated through the calcification of cyanobacterial filaments on grain surfaces (Kobluk and Risk 1977), or the precipitation of micrite within biofilms (Perry 1999). The very similar internal structure and thicknesses of these envelopes and the micritic ooid cortices suggest that they had the same, i.e., microbially mediated origin.

Discussion

The Early Triassic was a time of slow recovery of carbonate-producing organisms in marine systems after the greatest mass extinction in the history of the Earth (Erwin 2006). The post-Permian recovery was complex and uneven in different regions, depositional environments and marine biological communities, being controlled by various extrinsic (i.e., physical environment) and intrinsic (i.e., ecosystem dynamics) processes (Chen and Benton 2012; Wei et al. 2015). Several environmental stressors have been proposed for the Early Triassic including anoxia (or euxinia), global warming, hypercapnia, enhanced terrestrial sediment flux, eutrophication, and ocean acidification (Dineen et al. 2014; Bond and Grasby 2016). Closely associated with the mass extinction and subsequent environmental stresses is a wide array of unusual sedimentary facies and fabrics that are also referred to as anachronistic facies (Woods 2014). Such anomalous features are known

to have formed in several regions during the Early Triassic, i.e., the western, central and eastern Tethys, western and eastern Panthalassa, and the Boreal Seaway.

In a comprehensive review Woods (2014) distinguished three main groups of Lower Triassic anachronistic facies that are not exclusive of each other and may be largely overlapping: (1) microbialites; (2) features associated with enhanced precipitation of $CaCO_3$; and, (3) fabrics that form due to limited biologic activity. Following this classification, most of the identified AUCFs should be assigned to the second group while the vermicular limestone clearly belongs to the third group.

Enhanced precipitation of $CaCO_3$ occurred during the Early Triassic resulting in massive production of seafloor cements, cavity-fillings, and cements within microbialites (Woods 2014). The high levels of $CaCO_3$ supersaturation also promoted early cementation of the seafloor, which was coupled with a decline in bioturbation depths and intensity during the post-extinction recovery period (Twitchett and Wignall 1996; Wignall and Twitchett 1999; Pruss and Bottjer 2004a; Pruss et al. 2005a, b). Apparently, these factors were major controls on the deposition and preservation of the thin-bedded micritic limestones and limestone layers in the ribbon rock facies. They also favored the incipient lithification of thin carbonate beds and laminae that were ripped-up and reworked by storms to form the flat-pebble breccias/conglomerates and mud-chip conglomerates. Soft-sediment to brittle deformation seemingly triggered by paleoseismic activity was an important prerequisite for the generation of flat pebbles and mud chips, as well as the fragmentation of lithified lime mud layers in the ribbon rock facies.

The high degree of supersaturation of $CaCO_3$ together with the major loss of calcifying metazoans in the Early Triassic caused marine carbonate sedimentation to switch to predominantly abiotic and/or microbially mediated forms of precipitation (Kiessling et al. 2003; Payne et al. 2006). These two factors favored the widespread formation of ooids (Groves and Calner 2004) and also promoted microbialite calcification (Riding 2005). The thin stratigraphic interval with microbial oolites, compared to the occurrence of different ooid types in the overlying Spathian strata (Chatalov 2005, 2016), suggests temporary conditions indicative of a microbial bloom in very shallow, agitated waters. Therefore, apart from the unusual seawater chemistry and scarcity of metazoan biota, other factors must have also favored the short-lived formation of microbially coated grains. Woods (2013) presumed that high primary productivity driven by terrestrial runoff led to increasing production of microbial carbonate in nearshore settings favouring the growth of coated grains in the Virgin Limestone Mb. In the present case, such an assumption is plausible, taking into account the transgression of Tethyan waters onto continental areas with predominantly alluvial deposition towards the end of the Spathian (Chatalov 2016). The ooid formation was also affected by uniformitarian processes, i.e., wave agitation in warm shallow waters that promoted $CaCO_3$ precipitation due to CO_2 degassing.

Vermicular limestone belongs to the fabrics that form due to limited biologic activity related to the severity of the end-Permian mass extinction and/or persistent environmental stress (Woods 2014). The decrease of infaunal bioturbation during the Early Triassic was a consequence of harsh environmental conditions that dampened or prevented the recovery of trace makers (Twitchett and Wignall 1996; Wignall and Twitchett 1999; Pruss and Bottjer 2004a; Pruss et al. 2005a, b; Mata and Bottjer 2011). While the diversity of trace-fossil assemblages, burrow size and depth of bioturbation generally increased from earliest to late Early Triassic time (Pruss and Bottjer 2004a; Twitchett and Barras 2004; Chen et al. 2011; Zhao et al. 2015), these changes were asynchronous and variable in different geographic regions and depositional environments (see Hofmann 2016, and references therein). Locally stressful environmental conditions persisted in the late Early Triassic (Pruss and Bottjer 2004a; Zhao et al. 2008; Abbassi et al. 2015; Luo et al. 2016), or even in the early Middle Triassic (Jaglarz and Uchman 2010), resulting in the formation of vermicular limestones characterized by relatively low ichnodiversity, small burrow size, and reduced tiering. In the present case, the Spathian vermicular limestones may be attributed to enhanced lithification of the seafloor which prevented vertical burrowing, as well as shifting environmental conditions that limited the intensity of bioturbation, i.e., low oxygenation and/or elevated salinity of seawater. Therefore, this distinctive carbonate facies was formed due to both biotic processes, i.e., bioturbation, and environmental controls, i.e., harsh environmental conditions (Woods 2014).

The Spathian AUCFs examined here may be considered in the light of the 'Anachronistic Platform' model proposed by Woods (2009, 2014). This model describes the distribution of various types of Lower Triassic anachronistic facies across an idealized continental margin, distinguishing the contribution of chemical, biological, and sedimentary factors in their formation. Thus, only the microbial oolite facies can be clearly assigned to the 'intertidal to shallow subtidal environments' while the remaining facies are interpreted to have formed in 'middle to inner carbonate ramp environments' (Table 1). This interpretation is consistent with the observation presented above and previous sedimentological results concerning the Spathian carbonate successions in western Bulgaria (Belivanova 2000; Chatalov 2002, 2013; Chatalov et al. 2015). Accordingly, the general zonal distribution of the 'Anachronistic Platform' model can be confirmed.

An important aspect of this study is to specify whether the identified Spathian AUCFs represent genuinely anachronistic facies or simply unusual sedimentary features and

fabrics. Following the original definition of Sepkoski et al. (1991), the subtidal thin-bedded micritic limestones and flat-pebble breccias/conglomerates should be regarded as unequivocally anachronistic, taking into account their widespread distribution in Cambrian–Lower Ordovician and older strata (e.g., Sepkoski et al. 1991; Chen et al. 2009; Liu 2009; Gomez and Astini 2015; Smith et al. 2016; Wright and Cherns 2016). Likewise, the limestone-marl ribbon rocks greatly resemble Cambrian analogues, and therefore may be referred to as anachronistic facies. Ribbon rocks are abundant in many Lower Paleozoic successions but appear to decrease through the Middle Paleozoic (Brett et al. 2012). In addition, Lehrmann et al. (2001) noted the anachronistic reappearance of peritidal ribbon carbonates during the Early Triassic. Mud-chip conglomerates and vermicular limestones have been documented only from Lower to Middle Triassic rocks, and accordingly should be assigned to the group of unusual carbonate facies. This conclusion contradicts previous interpretations of mud-chip facies (Pruss et al. 2005b; Woods 2009) and vermicular limestones (Zhao et al. 2008; Woods 2014; Deng et al. 2016) as being anachronistic in nature. Moreover, the global distribution, unusual character, and occurrence during a distinctive period of time allow the vermicular limestones to be particularly defined as an example of time-specific facies (i.e., Brett et al. 2012). Micritic microbial ooids have not been widely reported from Precambrian and Lower Paleozoic rocks, and therefore, the Spathian microbial oolites studied herein should instead be regarded as an unusual facies.

Conclusions

The identified AUCFs in Spathian rocks from western Bulgaria include thin-bedded micritic limestone, flat-pebble breccia/conglomerate, mud-chip conglomerate, limestone-marl ribbon rock, vermicular limestone, and microbial oolite. Common characteristics of all facies are the absence or scarcity of skeletal remains and a very low amount of siliciclastic admixtures (except marl beds within the ribbon rocks). Formation of the AUCFs occurred in shallow subtidal settings as a result of three interacting factors, i.e., environmental conditions, biotic controls and actualistic sedimentary processes. The vermicular limestones belong to fabrics that formed due to limited biologic activity while the remaining AUCFs represent features that were related to enhanced precipitation of $CaCO_3$. Rapid early cementation of the seafloor (due to a high degree of $CaCO_3$ supersaturation) coupled with the absence of deep vertical bioturbation were major controls on the deposition and preservation of all facies except the microbial oolites. Locally stressful environmental conditions (i.e., fluctuating oxygen levels and/or salinity) contributed to the formation of vermicular limestones. Storm-induced currents and/or waves produced flat-pebbles and mud chips, while wave agitation along with a temporary microbial bloom favored the precipitation of micritic ooid cortices and constructive micrite envelopes around allochems. Primary deposition of the limestone-marl ribbon facies in a low-energy environment was controlled by periodic changes in terrigenous input (probably reflecting climate fluctuations). Paleoseismic activity played a presumably important role in the formation of the clast-bearing facies by causing soft-sediment to brittle deformation of thin carbonate layers. The closely associated thin-bedded micritic limestones, flat-pebble breccias/conglomerates and limestone-marl ribbon rocks correspond to the original definition of anachronistic facies, i.e., greatly resembling Precambrian and Lower Paleozoic analogues. In turn, the mud-chip conglomerates, vermicular limestones and microbial oolites are considered as simply unusual sedimentary features and fabrics. This study reports one rare occurrence of diverse Spathian AUCFs in subtidal settings with western Bulgaria being only the third documented region worldwide. The new results show that anomalous paleoceanographic conditions for carbonate sedimentation persisted locally in the shallow Western Tethys realm until late Early Triassic time. These atypical conditions were periodically favored during the Spathian by the interplay of global, regional and local controls.

Acknowledgements The co-operation of Y. Stefanov (Sofia University 'St. Kliment Ohridski') during the field work is greatly acknowledged. The insightful comments by Adam Woods (USA) and an anonymous reviewer helped to significantly improve the manuscript.

References

Abbassi N, Shabanian R, Golparvar RH (2015) Environmental impacts on the ichnofossil diversity of the lower part of the Elika Formation (Lower Triassic), Moro Mountain, NW Iran. Iran J Sci Technol 39(A3):273–280

Abdi A, Gharaie MHM, Bádenas B (2014) Internal wave deposits in Jurassic Kermanshah pelagic carbonates and radiolarites (Kermanshah area, West Iran). Sediment Geol 314:47–59

Abdolmaleki J, Tavakoli V (2016) Anachronistic facies in early Triassic successions of the Persian Gulf and its palaeoenvironmental reconstruction. Palaeogeogr Palaeoclimatol Palaeoecol 446:213–224

Bádenas B, Pomar L, Aurell M, Morsilli M (2012) A facies model for internalites (internal waves deposits) on a gently sloping carbonate ramp (Upper Jurassic, Ricla, NE Spain). Sediment Geol 271–272:44–57

Baud A, Richoz S, Marcoux J (2005) Calcimicrobial cap rocks from the basal Triassic units: western Taurus occurrences (SW Turkey). C R Palevol 4:501–514

Baud A, Richoz S, Pruss SB (2007) The Lower Triassic anachronistic carbonate facies in space and time. Glob Planet Change 55:81–89

Bayet-Goll A, Chen J, Moussavi-Harami R, Mahboubi A (2015) Depositional processes of ribbon carbonates in Middle Cambrian of Iran (Deh-Sufiyan Formation, Central Alborz). Facies 61:1–18

Belivanova V (2000) Triassic in the Golo Bardo Mountain—one example for the Balkanide facial type of Triassic in Bulgaria. In: Bachmann GH, Lerche I (eds) Epicontinental Triassic. Zbl Geol Palaeont Teil I, vol 9–10. Schweizerbart, Stuttgart, pp 1105–1121

Belivanova V, Chatalov A (2005) New data on the Middle Triassic complex of inner-ramp carbonate shoals in Western Bulgaria. C R Acad Bulg Sci 58:281–288

Benatov S, Chatalov A (2000) New data on the stratigraphy and lithology of the Iskar Carbonate Group (Lower–Middle Triassic) in the Zaburde district, Western Bulgaria. Ann Sofia Univ St. Kliment Ohridski Fac Geol Geogr 93:83–106 **(in Bulgarian)**

Blakey R (2011) Paleogeographic maps. Global paleogeography. Early to Middle Triassic (240 Ma). http://www2.nau.edu/rcb7/mollglobe.html. Accessed 1 April 2017

Bond DPG, Grasby SE (2016) On the causes of mass extinctions. Palaeogeogr Palaeoclimatol Palaeoecol 478:3–29

Brett CE, McLaughlin PI, Histon K, Schindler E, Ferretti A (2012) Time-specific aspects of facies: state of the art, examples, and possible causes. Palaeogeogr Palaeoclimatol Palaeoecol 367–368:6–18

Broglio Loriga C, Goczan F, Haas J et al (1990) The Lower Triassic sequences of the Dolomites (Italy) and Transdanubian Mid-Mountains (Hungary) and their correlation. Mem Sci Geol 42:41–103

Budurov K, Trifonova E, Zagorchev I (1995) The Triassic in southwest Bulgaria. Stratigraphic correlation of key sections in the Iskar Carbonate Group. Geol Balc 25:27–59

Čatalov G (1988) Ladinian-Karnian terrigenous invasion and the bifurcation of the Triassic carbonate platform in Bulgaria. C R Acad bulg Sci 41:99–102

Chatalov A (2000) Deformational structures in the Iskur Carbonate Group (Lower-Upper Triassic) from the Western Balkanides. Geol Balc 30:43–57

Chatalov A (2002) Inner ramp carbonate shoals from the Middle Triassic in Northwestern Bulgaria. Rev Bulg Geol Soc 63:3–20 **(in Bulgarian)**

Chatalov A (2005) Monomineralic carbonate ooid types in the Triassic sediments from northwestern Bulgaria. Geol Balc 35:63–91

Chatalov A (2013) A Triassic homoclinal ramp from the Western Tethyan realm, Western Balkanides, Bulgaria: integrated insight with special emphasis on the Anisian outer to inner ramp facies transition. Palaeogeogr Palaeoclimatol Palaeoecol 386:34–58

Chatalov A (2016) Global, regional and local controls on the development of a Triassic carbonate ramp system. Western Balkanides, Bulgaria. doi:10.1017/S0016756816000923

Chatalov A, Vangelov D (2001) Storm-generated deposits in the Anisian (Pelsonian) limestones from the Western Balkanides. Rev Bulg Geol Soc 62:11–23

Chatalov A, Stefanov Y, Vetseva M (2015) The Röt-type facies of the Western Balkanides revisited: depositional environments and regional correlation. Abstracts 31st IAS Meet Sediment Kraków, Polish Geol Soc, p 115

Chen ZQ, Benton MJ (2012) The timing and pattern of biotic recovery following the end-Permian mass extinction. Nat Geosci 5:375–383

Chen J, Chough SK, Chun SS, Han Z (2009) Limestone pseudoconglomerates in the Late Cambrian Gushan and Chaomidian Formations (Shandong Province, China): soft-sediment deformation induced by storm-wave loading. Sedimentology 56:1174–1195

Chen J, Han Z, Zhang X, Fan A, Yang R (2010) Early diagenetic deformation structures of the Furongian ribbon rocks in Shandong Province of China: a new perspective of the genesis of limestone conglomerates. Sci China Earth Sci 53:241–252

Chen Z, Tong J, Fraiser M (2011) Trace fossil evidence for restoration of marine ecosystems following the end-Permian mass extinction in the Lower Yangtze region, south China. Palaeogeogr Palaeoclimatol Palaeoecol 299:449–474

Chough SK, Kwon YK, Choi DK, Lee DJ (2001) Autoconglomeration of limestone. Geosci J 5:159–164

Colombié C, Schnyder J, Carcel D (2012) Shallow-water marl–limestone alternations in the Late Jurassic of western France: cycles, storm event deposits or both? Sediment Geol 271–272:28–43

Demicco RV, Hardie LA (1994) Sedimentary structures and early diagenetic features of shallow-marine carbonate deposits. Society of economic paleontologists and mineralogists atlas series 1, Society of Sedimentary Geology, Tulsa

Deng B, Wang Y, Woods A, Li S, Li G, Chen W (2016) Evidence for rapid precipitation of calcium carbonate in south China at the beginning of Early Triassic. Palaeogeogr Palaeoclimatol Palaeoecol 474:187–197

Dineen AA, Frasier ML, Sheenan PM (2014) Quantifying functional diversity in pre- and post-extinction paleocommunities: a test of ecological restructuring after the end-Permian mass extinction. Earth Sci Rev 136:339–349

Droser ML, Bottjer DJ (1986) A semiquantitative field classification of ichnofabric. J Sediment Pet 56:558–559

Einsele G, Ricken W (1991) Limestone–marl alternation: an overview. In: Einsele G, Ricken W, Seilacher A (eds) Cycles and events in stratigraphy. Springer, New York, pp 23–47

El Taki H, Pratt BR (2012) Syndepositional tectonic activity in an epicontinental basin revealed by deformation of subaqueous carbonate laminites and evaporites: seismites in Red River strata (Upper Ordovician) of southern Saskatchewan, Canada. Bull Can Pet Geol 60:37–58

Erwin DH (2006) Extinction: how life on Earth nearly ended 250 million years ago. Princeton University Press, Princeton

Ettensohn FR, Zhang C, Gao L, Lierman RT (2011) Soft-sediment deformation in epicontinental carbonates as evidence of paleoseismicity with evidence for a possible new seismogenic indicator: accordion folds. Sediment Geol 235:222–233

Ezaki Y, Liu J, Adachi N (2012) Lower Triassic stromatolites in Luodian County, Guizhou Province, south China: evidence for the protracted devastation of marine environments. Geobiology 10:48–59

Fang Y, Chen Z-Q, Kershaw S, Li Y, Luo M (2017) An Early Triassic (Smithian) stromatolite associated with giant ooid banks from Lichuan (Hubei Province), south China: environment and controls on its formation. Palaeogeogr Palaeoclimatol Palaeoecol. doi:10.1016/j.palaeo.2017.02.006

Flügel E (2004) Microfacies of carbonate rocks: analysis, interpretation and application. Springer, Berlin

Ganev M (1974) State of knowledge on the Triassic stratigraphy of Bulgaria. Stratigraphy of the Alpine-Mediterranean Triassic: symposium. Öster Akad Wissensch Schrift Erdwissen Kommis 2:93–99

Goff J, Chagué-Goff C, Nichol S, Jaffe BE, Dominey-Howes D (2012) Progress in palaeotsunami research. Sediment Geol 243–244:70–88

Gomez FJ, Astini RA (2015) Sedimentology and sequence stratigraphy from a mixed (carbonate–siliciclastic) rift to passive margin transition: the Early to Middle Cambrian of the Argentine Precordillera. Sediment Geol 316:39–61

Groves JR, Calner M (2004) Lower Triassic oolites in Tethys: a sedimentologic response to the end-Permian mass extinction. Geol Soc Am Ann Meet Abstracts with Programs 36:336

Haas J, Hips K, Pelikán P, Zajzon N, Götz AE, Tardi-Filácz E (2004) Facies analysis of marine Permian/Triassic boundary sections in Hungary. Acta Geol Hung 47:297–340

Hips K, Haas J (2006) Calcimicrobial stromatolites at the Permian-Triassic boundary in a western Tethyan section, Bükk Mountains, Hungary. Sediment Geol 185:239–253

Hips K, Pelikán P (2002) Lower Triassic shallow marine succession in the Bükk Mountains, NE Hungary. Geol Carp 53:351–367
Hofmann R (2016) The end-Permian mass extinction. In: Mángano MG, Buatois LA (eds) The trace-fossil record of major evolutionary events. Topics in geobiology, vol 39. Springer, Dordrecht, pp 325–349
Ivanov Z (1998) Tectonics of Bulgaria. Unpublished Professorship thesis. Sofia University St. Kliment Ohridski (in Bulgarian)
Jaglarz P, Uchman A (2010) A hypersaline ichnoassemblage from the Middle Triassic carbonate ramp of the Tatricum domain in the Tatra Mountains, Southern Poland. Palaeogeogr Palaeoclimatol Palaeoecol 292:71–81
Kiessling W, Flügel E, Golonka J (2003) Patterns of Phanerozoic carbonate platform sedimentation. Lethaia 36:195–225
Knaust D (2000) Signatures of tectonically controlled sedimentation in Lower Muschelkalk carbonates (Middle Triassic) of the Germanic basin. In: Bachmann GH, Lerche I (eds) Epicontinental Triassic. Zbl Geol Paläont Teil I, vol 9/10. Schweizerbart, Stuttgart, pp 893–924
Knaust D (2002) Pinch-and-swell structures at the Middle/Upper Muschelkalk boundary (Triassic): evidence of earthquake effects (seismites) in the Germanic Basin. Int J Earth Sci 91:291–303
Kobluk DR, Risk MJ (1977) Micritization and carbonate-grain binding by endolithic algae. Am Assoc Pet Geol Bull 61:1069–1082
Kullberg JC, Oloriz F, Marques B, Caetano P, Rocha RB (2001) Flat-pebble conglomerates: a local marker for Early Jurassic seismicity related to syn-rift tectonics in the Sesimbra area (Lusitanian Basin, Portugal). Sediment Geol 139:49–70
Lehrmann DJ, Wan Y, Wei JY, Yu YY, Xiao JF (2001) Lower Triassic peritidal cyclic limestone: an example of anachronistic carbonate facies from the Great Bank of Guizhou, Nanpanjiang Basin, Guizhou Province, south China. Palaeogeogr Palaeoclimatol Palaeoecol 173:103–123
Lehrmann DJ, Minzoni M, Li X, Yu M, Payne JL, Kelley BM, Schaal EK, Enos P (2012) Lower Triassic oolites of the Nanpanjiang Basin, south China: facies architecture, giant ooids, and diagenesis—implications for hydrocarbon reservoirs. Am Assoc Pet Geol Bull 96:1389–1414
Li F, Yan JX, Algeo T, Wu X (2013) Paleoceanographic conditions following the end-Permian mass extinction recorded by giant ooids (Moyang, south China). Glob Planet Change 105:102–120
Li F, Yan J, Burne RV et al (2017) Paleo-seawater REE compositions and microbial signatures preserved in laminae of Lower Triassic ooids. Palaeogeogr Palaeoclimatol Palaeoecol. doi:10.1016/j.palaeo.2017.04.005
Liu J (2009) Marine sedimentary response to the great Ordovician biodiversification event: examples from north China and south China. Paleontol Res 13:9–21
Łuczyński P, Skompski S, Kozłowski W (2014) Stromatoporoid beds and flat-pebble conglomerates interpreted as tsunami deposits in Upper Silurian of Podolia, Ukraine. Acta Geol Pol 64:261–280
Luo M, Chen ZQ, Zhao LS et al (2014) Early Middle Triassic stromatolites from the Luoping area, Yunnan Province, SW China: geologic features and environmental implications. Palaeogeogr Palaeoclimatol Palaeoecol 412:124–140
Luo M, George AD, Chen ZQ (2016) Sedimentology and ichnology of two Lower Triassic sections in south China: implications for the biotic recovery following the end-Permian mass extinction. Glob Planet Change 144:198–212
MacEachern JA, Pemberton SG, Gingras MK, Bann KL (2007) The ichnofacies paradigm: a 50-year retrospective. In: Miller W III (ed) Trace fossils: concepts, problems, prospects. Elsevier, Amsterdam, pp 52–77
Mata SA, Bottjer DJ (2011) Origin of Lower Triassic microbialites in mixed carbonate-siliciclastic successions: ichnology, applied stratigraphy, and the end-Permian mass extinction. Palaeogeogr Palaeoclimatol Palaeoecol 300:158–178
Mata SA, Bottjer DJ (2012) Microbes and mass extinctions: paleoenvironmental distribution of microbialites during times of biotic crisis. Geobiology 10:3–24
Miller MF, Smail SE (1997) A semiquantitative field method for evaluating bioturbation on bedding planes. Palaios 12:391–396
Montenat C, Barrier P, Ott d'Estevou P, Hibsch C (2007) Seismites: an attempt at critical analysis and classification. Sediment Geol 196:5–30
Mount JF, Kidder D (1993) Combined flow origin of edgewise intraclast conglomerates: Sellick Hill Formation (Lower Cambrian), South Australia. Sedimentology 40:315–329
Myrow PM, Tice L, Archuleta B, Clark B, Taylor JF, Ripperdan RL (2004) Flat-pebble conglomerate: its multiple origins and relationship to metre-scale depositional cycles. Sedimentology 51:973–996
Myrow PM, Chen J, Snyder Z, Leslie S, Fike DA, Fanning CM, Yuan J, Tang P (2015) Depositional history, tectonics, and provenance of the Cambrian-Ordovician boundary interval in the western margin of the North China block. Geol Soc Am Bull 127:1174–1193
Nawrocki J, Szulc J (2000) The Middle Triassic magnetostratigraphy from the Peri-Tethys basin in Poland. Earth Planet Sci Lett 182:77–92
Payne JL, Lehrmann DJ, Jiayong W, Knoll AH (2006) The pattern and timing of biotic recovery from the end-Permian extinction on the Great Bank of Guizhou, Guizhou Province, China. Palaios 21:63–85
Perry CT (1999) Biofilm-related calcification, sediment trapping and constructive micrite envelopes: a criterion for the recognition of ancient grass-bed environments? Sedimentology 46:33–45
Pruss SB, Bottjer DJ (2004a) Early Triassic trace fossils of the western United States and their implications for prolonged environmental stress from the end-Permian mass extinction. Palaios 19:551–564
Pruss SB, Bottjer DJ (2004b) Late Early Triassic microbial reefs of the western United States: a description and model for their deposition in the aftermath of the end-Permian mass extinction. Palaeogeogr Palaeoclimatol Palaeoecol 211:127–137
Pruss SB, Payne JL (2009) Early Triassic microbial spheroids in the Virgin Limestone Member of the Moenkopi Formation, Nevada, USA. Palaios 24:131–136
Pruss S, Fraiser M, Bottjer DJ (2004) Proliferation of Early Triassic wrinkle structures: implications for environmental stress following the end-Permian mass extinction. Geology 32:461–464
Pruss SB, Corsetti FA, Bottjer DJ (2005a) Environmental trends of Early Triassic biofabrics: implications for understanding the aftermath of the end-Permian mass extinction. In: Over DJ, Morrow JR, Wignall PB (eds) Understanding late devonian and Permian-Triassic biotic and climatic events: towards an integrated approach. Elsevier, Amsterdam, pp 313–332
Pruss SB, Corsetti FA, Bottjer DJ (2005b) The unusual sedimentary rock record of the Early Triassic: a case study from the southwestern United States. Palaeogeogr Palaeoclimatol Palaeoecol 222:33–52
Pruss SB, Bottjer DJ, Corsetti FA, Baud A (2006) A global marine sedimentary response to the end-Permian mass extinction: examples from southern Turkey and the western United States. Earth Sci Rev 78:193–206
Riding R (2005) Phanerozoic reefal microbial carbonate abundance: comparisons with metazoan diversity, mass extinction events, and seawater saturation state. Rev Esp Micropaleont 37:23–39
Rychliński T, Jaglarz P (2016) An evidence of tectonic activity in the Triassic of the Western Tethys: a case study from the carbonate succession in Tatra Mountains (S Poland). Carb Evap 32:103–116

Sepkoski JJ, Bambach RK, Droser ML (1991) Secular changes in Phanerozoic event bedding and the biological overprint. In: Einsele G, Ricken W, Seilacher A (eds) Cycles and events in stratigraphy. Springer, Berlin, pp 298–312

Smith EF, Macdonald FA, Petach TA, Bold U, Schrag DP (2016) Integrated stratigraphic, geochemical, and paleontological late Ediacaran to early Cambrian records from southwestern Mongolia. Geol Soc Am Bull 128:442–468

Szulc J (2000) Middle Triassic evolution of the northern Peri-Tethys area as influenced by early opening of the Tethys ocean. Ann Soc Geol Pol 70:1–48

Tronkov D (1968) The Lower-Middle Triassic boundary in Bulgaria. Bull Geol Inst Ser Paleont 17:113–131 **(in Bulgarian)**

Tronkov D (1973) Fundamentals of the Triassic stratigraphy in the Belogradchik antiklinorium (northwest Bulgaria). Bull Geol Inst Ser Strat Lithol 22:73–98 **(in Bulgarian)**

Tronkov D (1976) Triassic ammonite successions in the West Balkan Mountains of Bulgaria. C R Acad Bulg Sci 29:1325–1328 **(in German)**

Tronkov D (1981) Stratigraphy of the Triassic system in part of the West Srednogorie (West Bulgaria). Geol Balc 11:3–20 **(in Russian)**

Tronkov D (1983) Stratigraphic problems of Iskar Carbonate Group (Triassic) in South-west Bulgaria. Geol Balc 13:91–100 **(in Russian)**

Twitchett RJ, Barras CG (2004) Trace fossils in the aftermath of mass extinction events. In: McIlroy D (ed) The application of ichnology to palaeoenvironmental and stratigraphic analysis. Geological society london special publications, vol 228. Geological Society, London, pp 397–418

Twitchett RJ, Wignall PB (1996) Trace fossils and the aftermath of the Permo-Triassic mass extinction: evidence from northern Italy. Palaeogeogr Palaeoclimatol Palaeoecol 124:137–151

Vaptsarova A (1986) Lithological and facies characteristics of the Triassic rocks in Vlahina Mountains (southwest Bulgaria). Geol Balc 16:55–71 **(in Russian)**

Wei H, Shen J, Schoepfer SD, Krystin L, Richoz S, Algeo TJ (2015) Environmental controls on marine ecosystem recovery following mass extinctions, with an example from the Early Triassic. Earth Sci Rev 149:108–135

Westphal H, Hilgen F, Munnecke A (2010) An assessment of the suitability of individual rhythmic carbonate successions for astrochronological application. Earth Sci Rev 99:19–30

Wignall PB, Twitchett RJ (1999) Unusual intraclastic limestones in Lower Triassic carbonates and their bearing on the aftermath of the end-Permian mass extinction. Sedimentology 46:303–316

Woods AD (2009) Anatomy of an anachronistic carbonate platform: Lower Triassic carbonates of the southwestern United States. Aust J Earth Sci 56:825–839

Woods AD (2013) Microbial ooids and cortoids from the Lower Triassic (Spathian) Virgin Limestone, Nevada, USA: evidence for an Early Triassic microbial bloom in shallow depositional environments. Glob Planet Change 105:91–101

Woods AD (2014) Assessing Early Triassic palaeoceanographic conditions via unusual sedimentary fabrics and features. Earth Sci Rev 137:6–18

Wright VP, Cherns L (2016) How far did feedback between biodiversity and early diagenesis affect the nature of Early Palaeozoic sea floors? Palaeontology 59:753–765

Zhao XM, Tong JN, Yao HZ, Zhang KX, Chen ZQ (2008) Anachronistic facies in the Lower Triassic of south China and their implications to the ecosystems during the recovery time. Sci China Ser D Earth Sci 51:1646–1657

Zhao XM, Tong JN, Yao HZ, Niu ZJ, Luo M, Huang YF, Song HJ (2015) Early Triassic trace fossils from the Three Gorges area of south China: implications for the recovery of benthic ecosystems following the Permian-Triassic extinction. Palaeogeogr Palaeoclimatol Palaeoecol 429:100–116